Surrogate-Assisted Many-objective Optimization of Building Energy Management

Qiqi Liu, Felix Lanfermann, Tobias Rodemann, Markus Olhofer, Yaochu Jin

2023

Preprint:

This is an accepted article published in IEEE Computational Intelligence Magazine. The final authenticated version is available online at: https://doi.org/10.1109/MCI.2023.3304073

Surrogate-Assisted Many-objective Optimization of Building Energy Management

Qiqi Liu, Hebei University of Technology, CHINA and Bielefeld University, GERMANY
Felix Lanfermann, Tobias Rodemann, and Markus Olhofer, Honda Research Institute Europe, GERMANY
Yaochu Jin, Bielefeld University, GERMANY

***Abstract*—Building energy management usually involves a number of objectives, such as investment costs, thermal comfort, system resilience, battery life, and many others. However, most existing studies merely consider optimizing less than three objectives since it becomes increasingly difficult as the number of objectives increases. In addition, the optimization of building energy management relies heavily on time-consuming energy component simulators, posing great challenges for conventional evolutionary algorithms that typically require a large number of real function evaluations. To address the above-mentioned issues, this paper formulates a building energy management scenario as a 10-objective optimization problem, aiming to find optimal configurations of power supply components. To solve this expensive many-objective optimization problem, six state-of-the-art multi-objective evolutionary algorithms, five of which are assisted by surrogate models, are compared. The experimental results show that the adaptive reference vector assisted algorithm is proven to be the most competitive one among the six compared algorithms; the five evolutionary algorithms with surrogate assistance always outperform their counterpart without the surrogate, although the kriging-assisted reference vector assisted evolutionary algorithm only performs slightly better than the algorithm without surrogate assistance in dealing with the 10-objective building energy management problem. By analyzing the non-dominated solutions obtained by the six algorithms, an optimal configuration of power supply components can be obtained within an affordable period of time, providing decision makers with new insights into the building energy management problem.**

***Index Terms*—Evolutionary many-objective optimization, building energy management, real-world applications, surrogate-assisted evolutionary algorithms**

I. Introduction

The concept of reducing energy consumption to combat global warming has attracted increasing attention. In large building complexes such as campus and office buildings, a large amount of energy consumption is the everyday inevitability. Thus, managing the production, storage, and consumption in these complexes is of great importance. Investing into renewable energy like Photo Voltaic (PV) systems is, in this light, one of many options for improving the cost and emission performance of a facility. For facilities, like the Honda Research Institute, the investment in PV or battery systems has to consider a multitude of factors like investment costs, greenhouse gas emissions, profitability, grid stability, equipment (battery) lifetime, or system resilience. However, these objectives are usually conflicting. Moreover, with the involvement of different stakeholders, their preferences and trade-off for the factors should likewise be considered. Thus, the obtained solutions may not be applicable for implementation if some important objectives are not considered. As a result, many-objective optimization of the building energy management will be a highly desired alternative. A common approach to solving multi-objective problems (with two or three objectives) and many-objective problems (with more than three objectives) is to use multi-objective evolutionary algorithms (MOEAs), such as the non-dominated sorting genetic algorithm II (NSGA-II) [1], non-dominated sorting genetic algorithm III (NSGA-III) [2], multi-objective evolutionary algorithm based on decomposition (MOEA/D) [3], and reference vector assisted evolutionary algorithm (RVEA) [4], just to name a few.

Many researchers have proposed using canonical MOEAs to simultaneously optimize conflicting objectives within the context of building energy management to identify an optimal configuration of power supply components. For instance, the study in [5] endeavores to strike a balance between energy consumption cost and user satisfaction in home energy management. Meanwhile, the research in [6] proposes a strategy to shift the cooling load from peak to off-peak hours, thereby reducing energy costs to a certain extent without compromising thermal comfort. It should be noted that the majority of building energy management studies optimize no more than three conflicting objectives, since it is challenging for traditional optimization algorithms to strike a balance among more than three objectives.

As pointed out in [7], optimizing dwellings could take up to 12 days if MOEAs are used simply with the objective values from simulators such as EnergyPlus. This approach is not cost-effective for real-world applications, particularly for managing energy demand a day ahead, as discussed in [8]. Also, unpredictable environmental factors, such as weather changes, require the building energy management to react quickly. Thus, it is highly desired that the optimization of the building energy management is computationally efficient. During the past two decades, surrogate-assisted evolutionary algorithms (SAEAs) have shown to be highly successful in handling computationally expensive problems whose function evaluations can take from minutes to days to evaluate. While a few SAEAs have been proposed for expensive multi-objective problems (MOPs) and many-objective problems (MaOPs), it remains challenging to apply them to real-world applications.

Corresponding Author: Yaochu Jin (yaochu.jin@uni-bielefeld.de)

The first challenge is problem formulation, i.e., whether the formulation is reasonable or whether all essential factors are included for finding a solution for real implementation. Note that an inappropriate formulation could increase the difficulties of handling the problem. As discussed in [9], only by using a proper problem formulation, kriging-assisted reference vector guided evolutionary algorithm (K-RVEA) [10] could achieve an optimal solution that is much better than the baseline solution on the optimization of an air intake ventilation system.

Another challenge is that it can be hard to decide which algorithm should be adopted for a specific problem, especially for black-box problems whose properties are unknown. It is therefore highly desirable to conduct a comparative study of different algorithms when solving real-world applications. In addition, only a few simulation based expensive real-world applications with variable simulator runtime or many-objective properties have been reported in the past decade. In particular, a hybrid electric vehicle control problem with seven objectives [11], an automotive engine calibration problem with 10 objectives [12], and the design of radar waveforms with 10 objectives [13] are proposed, but each function of these three problems is relatively fast for evaluation. The proposed BEM problem in this work consists of 10 objectives with each function evaluation time ranging from seconds to minutes. It has the special property that the time for each function evaluation is different, and each function evaluation is expensive, so it is ideal for evaluating the performance of cost-aware Bayesian optimization. It should be noted that the performance of most cost-aware Bayesian optimization approaches such as [14]–[16] is merely tested on the single- or multi-objective optimization of the hyperparameters of neural networks because of a lack of real-world applications with variable simulator runtime for different function evaluations.

Considering the above-mentioned challenges and requirements, the contributions of this work are summarized as follows.

- This work identifies the need of the many-objective optimization for the BEM problem and proposes a 10-objective building energy management problem, carefully engineered around nine decision variables. This novel solution is tailored for a practical, real-world application on a German building complex, encompassing 10 meticulously designed objective functions. As an extension to our previous work [17] in which four conflicting objectives, i.e., investment cost, yearly energy costs, CO_2 emissions, and system resilience, are considered, we present six additional exemplary objectives that a decision-maker may take into account in identifying an optimal configuration of power system components.
- This work exemplifies a successful application of five multi-objective evolutionary algorithms with surrogate assistance (we call it multi-objective SAEAs hereafter for simplicity), and one without, i.e., traditional MOEA, to optimize the 10-objective BEM problem. By comparing these six algorithms, it is demonstrated that the five adopted multi-objective SAEAs could significantly improve the performance and efficiency, confirming the benefits of multi-objective SAEAs in handling time-consuming real-world applications.
- The proposed real-world many-objective BEM application with different evaluation costs can be used in the future for testing SAEAs or cost-aware Bayesian optimization algorithms.

The rest of this paper is organized as follows. Section II describes the related work on building energy management. Section III presents the formulation of BEM. Section IV studies the performance of the BEM system obtained by five multi-objective SAEAs and one MOEA. Section V concludes the paper.

II. Related Work

A. Work on Building Energy Management

The optimization of building energy management using SAEAs can be divided into two main categories, i.e., single-objective and multi-objective optimization. In the first group, the conflicting objectives are transformed into a single-objective optimization problem by weighting different objectives [6], [8], [18], [19] or treating some objectives as the constraints [20]. For instance, in [8] and [20], optimization is both conducted based on an artificial neural network using genetic algorithms. However, in [8], a single objective function is formulated by weighting energy cost and loading shifting, while in [20], it is formulated by using energy consumption as the objective function with thermal comfort as one of constraints.

In the second group, the conflicting objectives are simultaneously handled using MOEAs. For instance, in [21], four conflicting objectives, i.e., initial investment cost, running costs, CO_2 emissions, and system resilience are considered with the expectation of finding a suitable trade-off in terms of finance, environment, and system. All function evaluations are conducted using the SimulationX simulator. In [7], considering direct optimization based on the building energy simulation software EnergyPlus using NSGA-II is time-consuming, thus, parallel computing is adopted to reduce the computational cost. Some studies propose training a surrogate model, such as an artificial neural network, to replace real function evaluations from a simulator to reduce the computational cost. For instance, in [22], by training an artificial neural network to replace the real function evaluations, the trade-off between energy demand and thermal comfort can be efficiently achieved using canonical NSGA-II, multi-objective particle swarm optimization [23], and multi-objective genetic algorithm [24] as the optimizer, respectively. Same as in [22], NSGA-II is also used as the optimizer in [25], however, it aims at simultaneously meeting economic and environmental targets.

While leveraging a surrogate model in lieu of actual function evaluations that can enhance efficiency, some SAEAs designed for optimizing the BEM problem overlook the essential aspect of model management strategy, focusing solely on the constructed model. This oversight is evidenced in studies such as Delgarm et al. [22] and Xue et al. [25]. It is believed

that the model management strategy is of great importance to balance the exploitation and exploration during the search process as the initially built surrogate model may not be accurate. Only a few researchers study the improvement of the performance of building energy management by considering model management strategies. In [26], [27], all solutions obtained by the multi-objective particle swarm optimizer are evaluated by the EnergyPlus simulator at each round of surrogate update. In [28], kriging variance is used in the model management strategy to obtain a set of well-diversified and converged solutions. Note that the above-mentioned studies only consider the balance of two conflicting objectives in building energy management. In summary, only a few studies have been conducted on building energy management. As far as we know, very few of them have studied a many-objective scenario, of which only a maximum number of five objectives has been considered. However, many-objective optimization of the BEM is essential for solutions to be finally implemented in the real world.

B. Surrogate-Assisted Evolutionary Algorithms

In most evolutionary algorithms, it is assumed that the computation of objective values is relatively cheap and fast, i.e., the objective values can be quickly obtained, given any set of decision variables. Nonetheless, in certain applications, each function evaluation can be time-consuming. Therefore, the direct application of evolutionary algorithms to these computationally expensive problems will not be feasible due to the impracticality of performing a substantial number of real function evaluations. For instance, a single simulation run in computational fluid dynamics [9] or simulating a car crash [29] could take days to months. Different from traditional evolutionary algorithms, surrogate models can be built to partially replace the real objective function evaluations in SAEAs [30]. In SAEAs, apart from the surrogate construction, the strategy of model management or the acquisition function, plays a pivotal role. This strategy is used to determine the next query point to effectively improve the set of optimal solutions by well-balancing exploration and exploitation. An acquisition function is the function used to determine the next most suitable solution to be infilled using real function evaluation. Given that each real function evaluation is notably time-intensive for these expensive problems, the evolutionary optimization can be strategically applied to the acquisition functions. These computationally economical functions, offer a cost-effective solution, thereby conserving computational resources in SAEAs. The resulting optimal solution will then be evaluated using the real objective functions and the surrogates, such as Gaussian process models (GP, also called kriging), [31] will be updated.

Representative work of SAEAs for handling expensive MOPs and MaOPs can be mainly categorized into two groups. In the first group, a surrogate is built for each objective to represent the real objective function as in K-RVEA [10], kriging-assisted two-archive evolutionary algorithm (KTA2) [32], Euclidean distance based expectation improvement matrix (EIMEGO) [33], and MOEA/D assisted efficient global optimization (MOEA/D-EGO) [34]. The above-mentioned work seldom considers the PF shapes, while most recently, a kriging-assisted evolutionary algorithm, termed GP-iGNG [35], is proposed to solve problems with various Pareto front shapes, showing very promising results. Unlike the above-mentioned approaches, two optimization processes are performed in parallel in [36], instead of one, to optimize an amplified upper confidence bound in order to balance exploration and exploitation well. In the second group, instead of directly predicting the objective values, a surrogate is constructed to predict the dominance relationship. Classification-based surrogate-assisted evolutionary algorithm (CSEA) [37], dominance prediction assisted evolutionary algorithm [38], and the recent relation learning and prediction assisted evolutionary algorithm (REMO) [39] are part of the representative work. In this group, a classifier that is able to distinguish the relative quality of pairwise individuals is usually required, but the main difficulty is a lack of sufficient training data. To overcome this issue, a huge number of the training data is constructed by utilizing the pairwise relation between each two solutions [39], [40].

III. Problem Statement

The present optimization problem is an extended version of a real-world facility optimization problem, primarily targeting the reduction of energy costs and CO2 emissions. This revised version takes into account the incorporation of a PV system, a battery storage facility, and several pragmatic modifications to the heating system, bearing space constraints and cost factors in mind. The objectives presented in this work are derived from this analysis and represent different goals and concerns of facility management. The focus of the BEM problem is to pinpoint an optimal assembly of power supply components for an individual building. This building comprises various sections including office spaces, automotive testing benches, computer infrastructure, and other such facilities. Moreover, it includes a sensible combination of different investment options, such as a PV system, a battery storage, and a heat storage, as well as the respective controller settings. The different configurations are constructed by nine individual decision variables. The building also uses a combined heat and power (CHP) system, which is not optimized but needs to be considered for the calculation of the objectives. In total, 10 objectives, derived from the simulation output, contribute to the investment decision. These objectives are partially related and might not all be relevant in all related applications. However, they span a range of solution features that a decision-maker could potentially be concerned with.

A mathematical definition of a many-objective optimization problem is defined as follows.

$$\begin{cases} \min \mathbf{f}(\mathbf{x}) = (f_1(\mathbf{x}), f_2(\mathbf{x}), \cdots, f_M(\mathbf{x})), \\ \text{subject } to\ \mathbf{x} = (x_1, x_2, \ldots, x_D), x_i \in \mathbb{R}, \end{cases} \tag{1}$$

where $\mathbf{x}$ is a vector of D decision variables in the decision space $\mathbb{R}^D$. M is the number of objectives and $\mathbf{f}(\mathbf{x}) \in \Lambda \subset \mathbb{R}^M$ is the objective vector with M objectives, Λ is the objective space. When $M < 4$, (1) refers to a multi-objective optimization problem and when $M \geq 4$, (1) refers to a many-objective optimization problem.

TABLE I: The range of the decision variables. The hyphen symbol indicates that no unit is associated with the corresponding decision variable.

Parameter	Min value	Max value	Unit	Description	System component
α_{PV}	0	45	∘	PV inclination angle	PV system
β_{PV}	0	360	∘	PV orientation angle	PV system
P_{PV}	10	450	kW	PV peak power	PV system
C_B	5	1000	kWh	Battery capacity	Battery storage
$b_{SOC,max}$	0.50	0.95	-	Maximum battery SOC	Battery storage
$b_{SOC,min}$	0.05	0.40	-	Minimum battery SOC	Battery storage
P_{charge}	-500	149.9	kW	Battery charging threshold	Battery storage
$P_{discharge}$	150	700	kW	Battery discharging threshold	Battery storage
V_{CHP}	1	5	m^3	Heat storage volume	CHP

A. Description of the Decision Variables

The problem considers nine decision variables in total, which will be discussed in the following.

1) Inclination angle of photovoltaics system α_{PV} between $0°$ and $45°$.
2) Orientation angle of photovoltaics system β_{PV} between $0°$ and $360°$.
3) Installed peak power of the photovoltaics system P_{PV} between $10\,\mathrm{kW}$ and $450\,\mathrm{kW}$.
4) Nominal Battery Capacity C_B between $5\,\mathrm{kWh}$ and $1000\,\mathrm{kWh}$.
5) Maximum Battery state of charge $b_{SOC,max}$ between 0.50 and 0.95. The battery is charged only up to the specified maximum state-of-charge (SOC) to limit battery aging.
6) Minimum Battery state of charge $b_{SOC,min}$ between 0.05 and 0.40. The battery is discharged only down to the specified minimum SOC to limit battery aging. This excludes the emergency power supply.
7) Battery Charging Threshold P_{charge} between $-500\,\mathrm{kW}$ and $149.9\,\mathrm{kW}$. The stationary battery is charged when the current overall power demand is below the specified value.[1]
8) Battery Discharging Threshold $P_{discharge}$ between $150\,\mathrm{kW}$ and $700\,\mathrm{kW}$. The stationary battery is discharged when the current overall power demand is above the specified value.
9) Heat storage cylinder volume V_{Heat} between $1\,\mathrm{m}^3$ and $5\,\mathrm{m}^3$.

A summary of the decision variables and the affected system components is given in Table I. For the optimization framework, all parameters are normalized to the range 0 to 1.

B. Objective Function Description

A study comparing different many-objective optimization algorithms (without surrogate assistance) on this problem was conducted in [17]. However, this earlier study only focused on five independent objectives (the fifth objective battery life is not considered), whereas this work is targeting to evaluate 10 objectives in total. A summary of the objectives is given in Table II. As a prerequisite for the optimizer, all objectives need to be minimized. Note that hardware installation and other costs are based on data from 2019 and might have changed. The computation of objectives is based on the output of the simulation tool (for example, the grid electricity demand for every 15 min interval in the simulation time period). Also note that in contrast to many linearized simulation models that only employ analytical functions approximating the systems like the PV system or battery as in [41], our simulator can model even non-linear effects in high precision (at the cost of higher and variable simulation times).

1) Investment costs in Euro. In this paper, mainly three investment cost components are considered resulting from purchasing the PV system, the stationary battery, as well as the combined heat and power plant.

$$C_{invest} = I_{PV} + I_{Batt} + I_{HeatStor}, \tag{2}$$

where I_{PV}, I_{Batt}, and $I_{HeatStor}$ refer to the investment cost for the PV system, the stationary battery, and the heat storage tank, respectively. Linearly scaling cost factors are assumed for all three components ($1000\,\mathrm{Euro/kW}$ PV peak power, $250\,\mathrm{Euro/kWh}$ battery capacity, $700\,\mathrm{Euro/m^3}$ heat storage).
2) Annual operation costs in Euro per year. Maintaining and operating the whole system will involve the grid electric cost, the gas consumption, the peak electricity load cost and the CHP maintenance cost. Thus, these four costs constitute the annual cost.

$$C_{Annual} = C_{Grid} + C_{Gas} + C_{Peak} + C_{CHP}, \tag{3}$$

where C_{Peak} is the additional peak cost for the highest energy demand in a year. CHP maintenance costs of $4.3\,\mathrm{Euro}$ per hour of operation are assumed: a gas price of $0.025\,\mathrm{Euro/kWh}$ power demand from gas, a (beneficial) feed-in tariff of $0.07\,\mathrm{Euro/kWh}$ in case excess energy is fed into the grid, a (beneficial) subsidy of $0.087\,\mathrm{Euro/kWh}$ of energy produced by the CHP, a fixed base price of $1000\,\mathrm{Euro}$, and a price of $0.131\,\mathrm{Euro/kWh}$ for electricity provided from the grid. An additional amount of $100\,\mathrm{Euro/kW}$ is charged for the overall maximum power demand peak.
3) Yearly CO_2 emissions in tons. The CO_2 emissions are estimated based on the simulated electricity and gas

[1] A detailed description of the battery control approach can be obtained from [17].

consumption of grid electricity system, CHP, and boilers, respectively.

$$G_{total} = G_{grid} + G_{gas} \tag{4}$$

where G_{grid} is the amount of CO_2 emissions from grid electricity, approximated at $500\,\mathrm{g/kWh}$. The term G_{gas} refers to the amount of CO_2 emissions from operating the CHP and boilers, set at $185\,\mathrm{g/kWh}$.

4) Resilience in seconds. The term resilience refers to the duration the company would be able to operate in case no grid power is available, i.e., energy is only provided by local production (PV system and CHP) and battery energy storage. This is, for example, relevant in cases of severe mal-functions due to extreme weather conditions, malicious physical or cyber-attacks. The resilience is in our case computed as

$$R = \min\left(\frac{\mathbf{b}_{SOC} \cdot C_B}{\mathbf{P}_{load}}\right) \tag{5}$$

where $\mathbf{b}_{SOC}$ is the battery's state of charge vector (for all simulation time steps), C_B refers to the battery capacity and $\mathbf{P}_{load}$ is the grid load vector. Resilience thus refers to the minimum (of time) over all 15 min time periods in the simulation of energy in the battery $(b_{SOC}(t) * C_B)$ divided by the respective power consumption $P_{Load}(t)$. This can be interpreted as the time period, for which the company would still be able to operate all electric components, at the worst point in time, i.e., the lowest ratio of battery state of charge and current electric load. Since all objectives need to be minimized, Equation (5) is formulated negatively as

$$R' = -R \tag{6}$$

5) Mean battery state of charge $\bar{b}_{SOC}$, between 0 and 1: $\bar{b}_{SOC}$ is the average state of charge of the stationary battery over the entire simulation. On one hand, a high mean state of charge enables the battery to discharge large amounts of energy to mitigate high peak costs when the overall power consumption is high. However, on the other hand, a high battery SOC over large periods of time is undesirable, as it leads to faster battery degradation.
6) Yearly energy discharged from battery $E_{batt,discharge}$ in kWh. A second indicator for battery degradation is the amount of energy that is discharged from it. The more energy discharged (and charged) from it, the faster the degradation.
7) Maximum power peak $P_{peak,supply}$ in kW. The maximum power demand peak is treated as an individual objective. Aside from contributing to higher annual costs due to peak demand charges for the customer, a high maximum power peak may lead to instability of the grid.
8) Time share t_m between 0 and 1 of the time in which the battery SOC is between 30% and 70%. As a trade-off between battery degradation and the ability to react to high demand charges, this objective creates an additional incentive to charge the battery with a medium amount of energy. Since the objectives are minimized to an intermediate charge (SOC) level, it is formulated as

$$t'_m = 1 - t_m \tag{7}$$

9) Yearly energy E_{feed} fed into the grid in kWh. Minimizing the amount of energy that is fed into the grid has multiple advantages. It maximizes PV power self-consumption and creates a higher level of independence from the energy supplier. It also reduces CO_2 emissions and leads to lower annual costs, since the feed-in tariff is lower than the grid supply rate. Yearly energy E_{feed} is already included in objective annual operation costs, but might be of special interest for some decision makers.
10) Maximum feed-in power peak $P_{peak,feed}$ in kW. Similar to the previous objective, a lower maximum feed-in power peak relates to higher PV power self-consumption and generally an efficient usage of self-produced energy. Furthermore, penalizing the maximum feed-in peak might be a realistic option for the supplier to reduce grid instability and frequency issues in the future. This would create additional costs for the consumer. In the present cost structure, there is no monetary impact of $P_{peak,feed}$, but due to its impact on the grid stability, it is, however, also considered as a separate objective.

In BEM, all decision values have an impact on the internal electricity consumption (vector over time) of the building that is simulated and all objectives (except for C_{invest}) are affected by this consumption, either directly (like C_{annual}) or indirectly via the amount of energy that is stored in the stationary battery, or when this energy is discharged. Sensitivity analysis between the decision variables and all objectives is carried out, which confirms that nine of the ten objectives are affected by all decision variables, except that C_{invest} is determined by P_{PV}, C_B, and $b_{SOC,max}$ only. The details of the sensitivity analysis are not provided here due to space limit. In summary, the simulation setup offers multiple directions to consider when optimizing the configuration. A large PV system enables the building to produce a significant share of the overall used energy, keeping the annual costs, peak power, and emissions low, while at the same time requiring a high initial investment. Orientation and inclination of the PV system can be tuned to define at which points in time (daily and seasonal) the system produces the most power. A large battery is also costly, though advantageous with regard to resilience and supply power peak. Many of the objectives are very sensitive to the four parameters that define the operation of the battery ($b_{SOC,max}$, $b_{SOC,min}$, P_{charge}, $P_{discharge}$) and therefore, create a challenging optimization task.

IV. Methods

A. Adopted Algorithms

Five multi-objective SAEAs, i.e., GP-iGNG, RVMM, K-RVEA, KTA2, and REMO, and one MOEA, i.e., RVEA-iGNG, are adopted to optimize the BEM problem. RVEA-iGNG is

TABLE II: Objective description and range. The hyphen symbol indicates that no unit is associated with the corresponding objective, or that there is no upper or lower bound.

Objective	Min value	Max value	Unit	Description
C_{invest}	0	-	Euro	Investment costs
C_{annual}	0	-	Euro	Operation costs
G_{total}	0	-	t	CO_2 emissions
R'	-	0	s	(negative) Resilience
$\bar{b}_{SOC}$	0	1	-	Mean battery SOC
$E_{batt,discharge}$	0	-	kWh	Discharged energy
$P_{peak,supply}$	0	-	kW	Supply power peak
t'_m	0	1	-	Medium SOC share
E_{feed}	0	-	kWh	Feed-in energy
$P_{peak,feed}$	0	-	kW	Feed-in power peak

used to verify whether SAEAs can converge faster than the traditional MOEA with the help of cheap surrogates and a model management strategy. Before discussing the detailed mechanism of the six algorithms, this study first illustrates how a multi-objective SAEA is different from an MOEA. In multi-objective SAEAs, the function evaluation is partly conducted on the built cheap surrogate model. This way, the computational cost can be reduced immensely when the real objective function is time-consuming. Note that the optimization process is partly based on the predicted objective values instead of the real objective values, so a reliable surrogate model is highly desired, which usually relies on an efficient surrogate model management strategy. A brief introduction of the six algorithms is as follows.

1) GP-iGNG [35]. GP-iGNG is able to handle expensive problems with various kinds of Pareto front shapes, making it suitable for handling real-world applications whose Pareto fronts are not known beforehand.
2) RVMM [36]. An adaptive reference vector based model management strategy is proposed. By optimizing an amplified upper confidence bound acquisition function using two optimization processes on top of two sets of reference vectors, RVMM shows great competitiveness in handling expensive many-objective problems.
3) K-RVEA [10]. The optimization is conducted on the basis of the predicted mean values of GP models, and the selection of newly infilled solutions is based on the angle penalized distance and the uncertainty.
4) KTA2 [32]. Three Gaussian process models, i.e., one global GP model and two GP influential point-insensitive models, are proposed to improve the prediction accuracy. An adaptive acquisition function that can adaptively emphasizing convergence, diversity or uncertainty is proposed in KTA2.
5) REMO [39]. Different from regression-based SAEAs, a neural network based relation model is trained to learn the relationship between pairs of candidate solutions.
6) RVEA-iGNG [42]. RVEA-iGNG is an MOEA that is proposed to handle many-objective problems. RVEA-iGNG is based on the framework of reference vector assisted evolutionary algorithm (RVEA), and the reference vectors are adjusted by training an improved growing neural gas network. Given the absence of *a prior* knowledge regarding the shape of the true Pareto fronts of the BEM problem, RVEA-iGNG proves to be an appropriate choice. This is due to its competitive performance in handling benchmark problems characterized by various types of Pareto fronts. It is worth mentioning that other state-of-the-art MOEAs can also be used.

To sum up, the five adopted SAEAs differ in the following aspects.

- Model construction. In GP-iGNG, RVMM, and K-RVEA, a traditional GP is adopted as the surrogate model for each objective to replace in part the objective function. KTA2 overcomes the drawbacks of conventional GPs by excluding those influential points from the training set and constructs three separate GP models. In REMO, one relation model is constructed using a neural network to learn the relationship between pairs of solutions.
- Model management strategy. In GP-iGNG, KTA2, and K-RVEA, the model management strategies are different, although they are all based on the solution set obtained by one optimization process using the GP models as the approximated objectives. In RVMM, the exploration and exploitation are balanced by selecting solutions from two optimization processes, each accounting for convergence and diversity, respectively. In REMO, the model management strategy is based on a specific voting strategy, and solutions with higher scores will be evaluated using the real function evaluations.

V. Experimental Results

A. Parameter Settings

For the five multi-objective SAEAs and one MOEA, the maximum number of real function evaluations is set to 1000 and 11200, respectively. The population size for the five adopted algorithms is set to 230. The initial number of training data for the five multi-objective SAEAs is set to $11 \cdot D - 1$, where D is the dimension of the decision space. The initial $11 \cdot D - 1$ real function evaluations contribute to the maximum number of 1000 or 11200 real function evaluations. In this paper, the five adopted multi-objective SAEAs are conducted for 10 independent runs and the adopted MOEA, i.e., RVEA-iGNG, is conducted for six independent runs due to time limitations.

B. Performance Indicator

In this study, hypervolume (HV) [43] is adopted as the performance indicator since the true Pareto front (PF) for the BEM problem is not known. The reference point for calculating HV is obtained by all the non-dominated solutions obtained by the five algorithms under comparison.

$$H(S) = \wedge\Big(\bigcup_{p\in S, p\leqslant r} [p, r]\Big) \tag{8}$$

where $\wedge$ denotes the Lebesgue measure, and $[p, r] = \{q \in \mathbb{R}^d | p \leqslant q \text{ and } q \leqslant r\}$ denotes the box delimited below by $p \in S$ and above by r. The HV contribution of a point to a set $p \in \mathbb{R}^d$ is as follows:

$$H(p, S) = H(S) - H(S \setminus p) \tag{9}$$

A reference point is required for HV calculation. As discussed in [44], [45], first the non-dominated solutions by the six algorithms are normalized using the ideal point and nadir point (which are the minimum and the maximum objective value of each objective of all non-dominated solutions). Then, the HV values of all normalized solutions can be calculated using the reference point $(1.1, 1.1, ..., 1.1)$.

C. Employed Simulation System and Optimization Framework

The energy management system is simulated using the commercial tool SimulationX[2], which is based on the Modelica simulation language[3] (Fig. 1). The adopted SimulationX simulator can create a complete renewable energy system rather than some components only, as shown in Fig. 1. The hybrid simulation approach employs sensor readings from a real facility and well tested simulation modules based on fundamental physical equations. The simulation model was built based on an analysis of the real building and smart meter measurements of real energy consumption over several years. The aggregated simulation output, like yearly energy consumption, has been validated against real consumption values. More information on the simulation approach can be found in [46]. Building energy consumption profiles and weather patterns are based on recorded energy consumption values of real buildings obtained by smart meter measurements. Modelica uses differential equations (DE) of the underlying physical processes to simulate technical elements like PV systems or batteries. Different levels of details can be simulated, including non-linear effects like variable technical efficiencies, which are often not represented in simpler simulation approaches. The drawback of this modeling approach is an increased runtime, which is also additionally dependent on the specific characteristics of the simulated system (due to the way the internal DE solver works). For example, simulating the (otherwise) same system with two different battery sizes might take different times. Certain extreme conditions (especially those that no human engineer has ever considered) might even cause the simulation run to stall completely. It is therefore necessary to stop long-running simulations when runtime exceeds a certain threshold (as will be discussed in more detail in Section IV. E) and discard this solution (by setting all objectives to the worst possible level). If this time-out threshold is set properly, the impact on the overall simulation results was found to be low.

[2]https://www.esi-group.com/products/system-simulation
[3]https://modelica.org/modelicalanguage.html

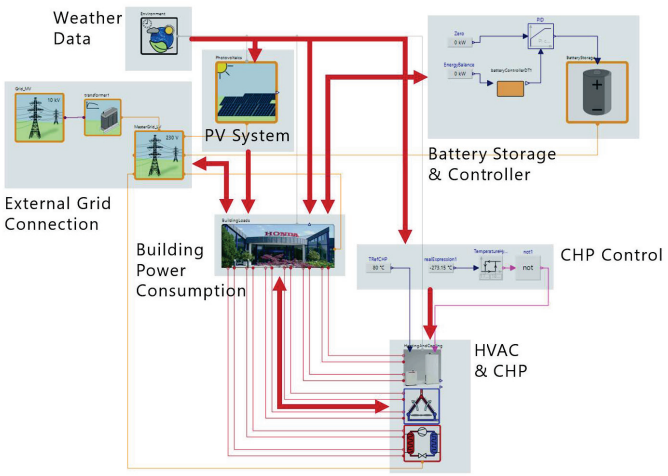

Fig. 1: A system view of the simulation: The model simulates the building power and heat demand based on time and weather conditions. Energy is provided by the grid connection, a PV system, a combined heat and power plant (CHP), and a stationary battery. The battery's charging and discharging behavior is controlled depending on a predetermined control strategy and internal reference values, e.g., the overall power consumption level.

Generally, the configuration needs to be evaluated based on the simulation of at least a complete year (to cover all seasons). However, this work first conducts the optimization based on a single month to have sufficient runs for a fair comparison of algorithms. The month of August is chosen in this work, as it shows the most similar results compared to a full year in previous studies. Since the overall system can be influenced by different seasons, e.g., sunshine and temperature, in future work, we would study the performance of the algorithms on the optimization of the BEM over a complete year.

Regarding the optimization tool, the six adopted algorithms under comparison are all implemented under the PlatEMO framework [47] to optimize the BEM application.

D. Performance Comparison of the Six Algorithms

To further substantiate the potential of surrogate models and efficacious model management strategies in enhancing algorithmic performance, a comparative analysis is conducted. This analysis examines the performance of five multi-objective SAEAs, namely, GP-iGNG, KTA2, K-RVEA, REMO, and RVMM, juxtaposed with a traditional MOEA - RVEA-iGNG, in the context of the BEM optimization. In Fig. 2, the HV values of the solutions obtained by the six algorithms over the 1000 real function evaluations are given. It can be seen that RVMM achieves the best HV value among the five algorithms,

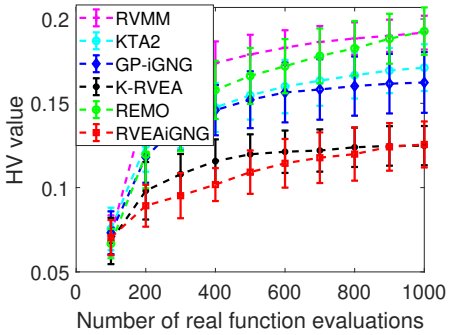

Fig. 2: The mean HV curve over the number of real objective function evaluations obtained by the six adopted algorithms over the evolution process. The upper and lower bars denote the standard deviation over 10 runs.

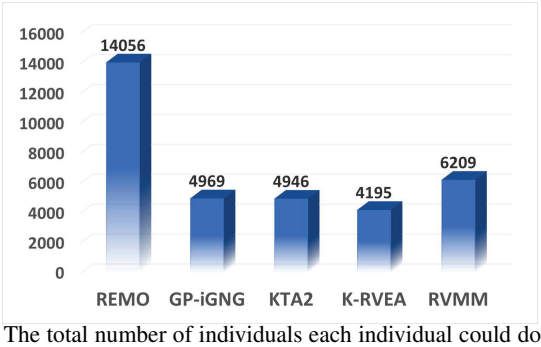

Fig. 3: The total number of individuals each individual could dominate within the optimal solution set obtained by each of the five SAEAs.

followed by REMO and KTA2. Overall, REMO and RVMM achieve similar performance over the number of real function evaluations. GP-iGNG performs slightly worse than KTA2. RVEA-iGNG, one of the MOEAs without surrogate assistance, performs only marginally worse than the state-of-the-art K-RVEA in dealing with BEM. In Fig. 3, We calculate the total number of individuals each individual could dominate within the optimal solution set obtained by each of the five SAEAs. The result is almost consistent with the HV results, showing that the number of solutions obtained by REMO is the largest,

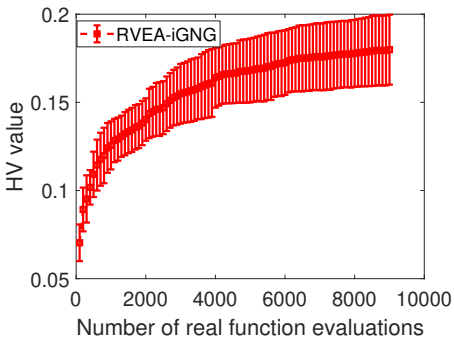

Fig. 4: The HV curve over the number of real objective function evaluations obtained by RVEA-iGNG over six independent runs. Note that the abnormal solutions are deleted before calculating the HV values. Thus, the number of the existing solutions is less than 11200.

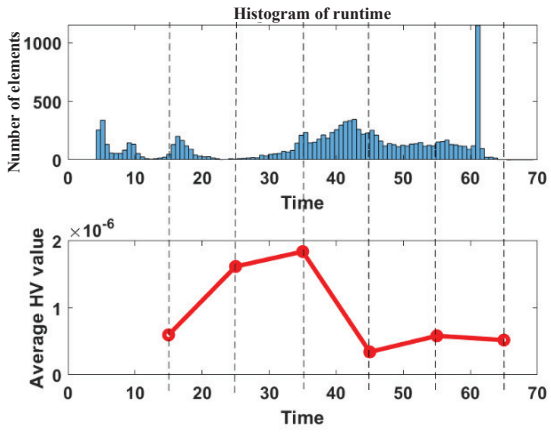

Fig. 5: Histogram of the runtime

followed by RVMM.

To observe the degree of improvement of the five multi-objective SAEAs in handling BEM, compared with RVEA-iGNG, we conduct the test on BEM using RVEA-iGNG with a maximum number of 11200 real function evaluations. In Fig. 4, it is observed that the performance of RVEA-iGNG increases sharply over the first 4000 real function evaluations and then increases at a slower pace until the exhaustion of the 11200 real function evaluations budget. The mean HV values obtained by RVMM, REMO, KTA2, GP-iGNG, and K-RVEA with a maximum of 1000 real function evaluations, and RVEA-iGNG with a maximum of 11200 real function evaluations are 0.1928, 0.1919, 0.1712, 0.1623, 0.1249, and 0.1804, respectively. It can be concluded that RVMM and REMO can converge almost 10 times faster than RVEA-iGNG. The HV values of the solutions obtained by RVMM and REMO with a maximum number of 1000 real function evaluations, i.e., 0.1928 and 0.1919, surpass the HV value of the solutions obtained by RVEA-iGNG with a maximum number of 11200 real function evaluations, i.e., 0.1804. It is noteworthy that REMO and RVMM, when compared to the other three multi-objective SAEAs, demonstrate significantly superior performance in the context of the BEM optimization. The HV values of the solutions obtained by KTA2 and GP-iGNG with a maximum number of 1000 real function evaluations, i.e., 0.1712 and 0.1623, are close to that obtained by RVEA-iGNG with a maximum number of 11200 real function evaluations, i.e., 0.1804.

E. Runtime and Timeout Analysis

Conventional MOEAs necessitate a considerable quantity of real function evaluations. Therefore, when each evaluation is time-intensive, it restricts the feasible number of real function evaluations that can be feasibly carried out. In this study, RVEA-iGNG is applied to optimize the BEM with a maximum number of 11200 real function evaluations, and one independent run takes about six days. It takes around 65 hours for the five adopted multi-objective SAEAs with a maximum number of

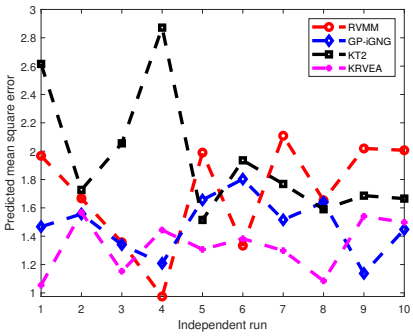

Fig. 6: Mean squared prediction error of surrogates for all objectives over 10 independent runs.

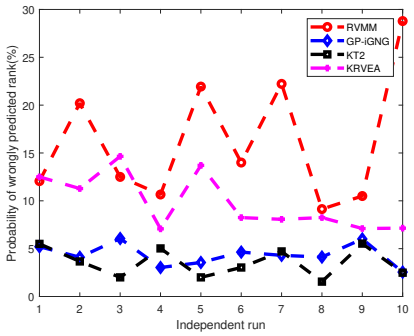

Fig. 7: Probability that a solution's Pareto dominance rank is wrongly predicted over 10 independent runs.

1000 real function evaluations. During the simulation of the BEM, each evaluation may take a few seconds to minutes. Thus, in this subsection, the histogram of the evaluation time of the 11200 real function evaluations is shown in Fig. 5 to illustrate the distribution of the evaluation time. It is observed that the most frequent evaluation time is in the range of about 35 seconds to 65 seconds.

Currently, the optimization is merely conducted based on the data from the month of August, and the evaluation time ranges from seconds to hours for different sets of decision variables, which is not affordable for traditional MOEAs. During the experiments, it is observed that the time of one function evaluation could be up to hours for some sets of decision variables. Therefore, we first record the simulation time for each function evaluation and then set the maximum time limit to 7200 seconds, i.e., if the simulation time of one solution is longer than 7200 seconds, then this solution will be abandoned to improve the efficiency of optimization. It is observed that a number of solutions take more than 7200 seconds, while for the majority of solutions, the time it takes is in the range of 0 to 70 seconds.

To analyze in which time range the solutions are more beneficial to the optimization process, those solutions whose time is longer than 70 seconds are first removed and then the HV contribution of solutions whose simulation time is below 70 seconds (s) is studied. We divide the whole evaluation time into six sub-ranges, i.e., 0 to 15s, 15 to 25s, 25 to 35s, 35 to 45s, 45 to 55s, 55 to 65s, and study the HV contribution of the solutions in each sub-range, as shown in Fig. 5. It can be seen that the solutions in the range of 15 to 35 seconds contribute the most to the HV values, and solutions in the range below 15 and above 35 contribute less. It is concluded that the reasonable timeout value shall not be set to less than 35 seconds if we want to speed up optimization process. Note that long simulation times are also often an indicator of numerical instabilities, which makes a removal of these solutions even more advisable.

F. Analysis of the Surrogate Accuracy

Both surrogate model and model management constitute critical factors that significantly influence the performance of multi-objective SAEAs. Note that in Fig. 2, RVMM performs the best in terms of HV value, followed by REMO, while K-RVEA ranks the worst. REMO adopts a neural network to predict the relationship between pairs of solutions instead of the objective values as in GP. Considering it is difficult to make comparisons of accuracy between the neural network and GP surrogates, only the accuracy of GP surrogates in four GP-assisted evolutionary algorithms is analyzed in this subsection. To better compare the adopted algorithms in solving BEM, we study the model accuracy of GPs trained by a subset of the solution set obtained by each algorithm under comparison. 80 percent of solutions are selected as training data and 20 percent as the test data. The solutions' objective values are first predicted using the constructed GP models to obtain the predicted objective values, and then they are compared with their real objective values. The mean squared errors between the predicted objective values and real objective values are plotted in Fig. 6. Interestingly, it is observed that the prediction error of the solution set obtained by K-RVEA is overall the lowest among the four multi-objective SAEAs under comparison. Specifically, RVMM, GP-iGNG, KTA2, and K-RVEA win on four, one, zero, and five out of 10 independent runs in terms of the prediction error. In addition to the predicted mean squared error, we also calculate the probability that a solution's Pareto dominance rank is wrongly predicted, considering that in multi- or many-objective optimization, the rank, instead of the objective values of a solution, is used to determine the quality of the solution. Fig. 7 shows that KTA2 and GP-iGNG predict the rank more accurately than K-RVEA and RVMM. Interestingly, RVMM occupies the lowest position in terms of rank prediction. This finding suggests that diminished model accuracy does not invariably equate to a decline in the performance of multi-objective SAEAs. Since in RVMM, two GPs are constructed in parallel in two optimization processes, and the low mean accuracy of two GPs may result from two GPs serving different purposes in two optimizations, i.e., one emphasizing on accelerating the convergence and the other on diversity. Note that in K-RVEA and GP-iGNG, the optimization process in both algorithms is based on the predicted mean values of a constructed GP model, supporting the statement that apart from the constructed surrogate model, model management

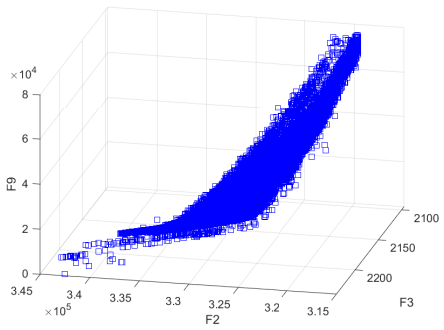

Fig. 8: The approximated Pareto front of the second objective (F2), the third objective (F3), and the ninth objective (F9).

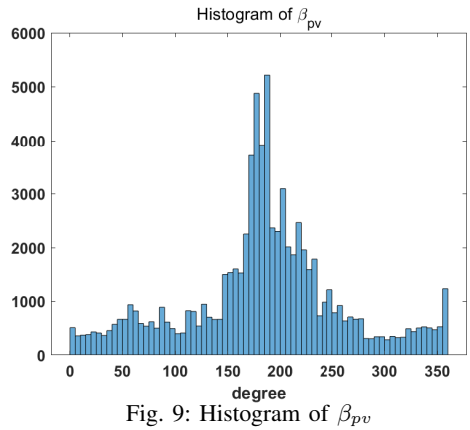

Fig. 9: Histogram of β_{pv}

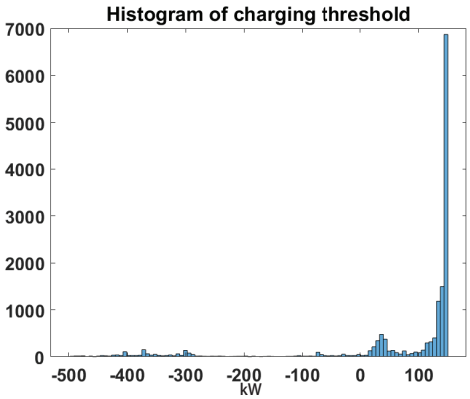

Fig. 10: Histogram of charging threshold

strategy is vital in guiding the search process.

G. Property Analyses of the BEM Problem

As previously discussed, certain solutions might be inherently unstable in real-world scenarios, leading to high time resolutions in simulations. Consequently, even after a waiting period of 7200 seconds, the computation of objective values might remain incomplete. Also, apart from the expensive property of this BEM problem, Fig. 5 shows that the runtime for different objectives is also different.

Take the second, third, and ninth objective of the non-dominated solutions as an example, as shown in Fig. 8, the shape of the obtained Pareto front is further analyzed. As defined in [48], a Pareto front is called regular if an infinite number of vectors with positive directions all intersect with it; otherwise, it is irregular. It is observed that the approximated Pareto front in Fig. 8 only covers a small part of the whole objective space. Thus, it is concluded that the approximated Pareto front of this BEM problem is irregular. This irregular Pareto front property could possibly explain the ineffectiveness of K-RVEA in handling BEM, in which a set of predefined evenly distributed reference vectors covering the whole objective space is adopted.

H. Analysis of the Solutions

To better visualize the solutions obtained by the six algorithms, both the decision variables and the objective values of the obtained non-dominated solutions are illustrated. For the PV system, the orientation angle of the photovoltaics system is around 180 degrees in most cases, which means it is southward, as confirmed in Fig. 9. The few northward facing PV-systems can be explained by the configurations with very small PV peak-powers. For those solutions, the orientation and inclination have no impact on the result, as they do not contribute to the energy production.

Fig. 10 shows that for most solutions, the battery is charged when the surplus power is above 149.9 kW (which is the upper limit of the parameter). Essentially, a higher charging threshold seems to be more reasonable. For the discharging limit in Fig. 11, it is observed that there are multiple reasonable values, although many of the solutions are around 300 kW.

We now study the correlation between objectives (for better visualization only pairwise comparisons are considered). In Fig. 12, only two dimensions of the 10-dimension objective values of the non-dominated solutions are plotted, and it is observed that there is a (rather weak) negative correlation between the investment costs and the annual operation costs. Similarly, in Fig. 12, the investment costs and the yearly CO_2 emissions are also negatively correlated, as expected. However,

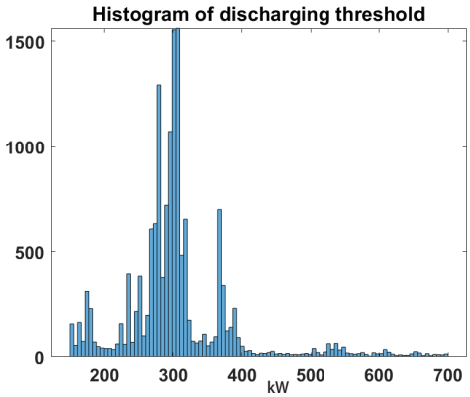

Fig. 11: Histogram of discharging threshold

TABLE III: The best found solution by all runs of the five algorithms for each objective and the objective values of two additional knee points.

id	best	C_{invest}	C_{annual}	G_{total}	R	b_{SOC}	$E_{batt,discharge}$	$P_{peak,supply}$	t_m	E_{feed}	$P_{peak,feed}$
1	C_{invest}	11600.00	335855.99	2156.36	-3.83	0.3623	1024.46	333428.19	0.3324	0.00	0.00
2	C_{annual}	566695.73	318833.10	2091.74	-1004.80	0.2000	0.01	333428.19	1.0000	76409.66	310735.30
3	G_{total}	566695.73	318833.10	2091.74	-1004.80	0.2000	0.01	333428.19	1.0000	76409.66	310735.30
4	R	666050.99	322715.73	2106.34	-9086.84	0.8828	8199.41	333429.00	0.9896	50683.61	226282.66
5	b_{SOC}	315240.88	326323.42	2120.30	-47.95	0.0274	328.24	333428.21	1.0000	20415.92	107002.88
6	$E_{batt,discharge}$	11600.01	335854.46	2156.44	-10.80	0.2000	0.00	333428.19	1.0000	0.00	0.00
7	$P_{peak,supply}$	106201.35	336393.05	2158.40	-431.47	0.6387	111547.83	273239.52	0.7589	0.00	0.00
8	t_m	253864.20	333533.27	2147.19	-874.72	0.5971	654.20	333428.19	0.0002	0.00	0.00
9	E_{feed}	566335.20	331701.31	2140.57	-6294.54	0.9205	6344.97	333432.17	0.9871	0.00	0.00
10	$P_{peak,feed}$	344858.68	337084.61	2154.64	-526.49	0.1040	494.72	333428.20	1.0000	0.00	0.00
11	(knee point 1)	460329.69	330866.87	2137.58	-7842.71	0.7223	6150.24	333428.35	0.9879	2843.12	26893.59
12	(knee point 2)	375578.36	330794.14	2137.21	-8153.59	0.7861	6956.20	333428.79	0.9878	7533.43	46370.87

TABLE IV: The best-found solution by all runs of the five algorithms for each decision variable and the decision values of two additional knee points.

id	best objective	α_{PV}	β_{PV}	P_{PV}	C_B	$b_{SOC,max}$	$b_{SOC,min}$	P_{charge}	$P_{discharge}$	V_{CHP}
1	C_{invest}	33.63	57.25	10.00	5.00	0.5000	0.0716	149.87	278.83	4.8401
2	C_{annual}	45.00	185.49	450.00	465.32	0.5200	0.3681	-431.47	698.76	4.9332
3	G_{total}	45.00	185.49	450.00	465.32	0.5200	0.3681	-431.47	698.76	4.9332
4	R	34.65	216.24	415.43	1000.00	0.8883	0.3606	45.10	629.54	4.8264
5	b_{SOC}	18.98	199.38	270.19	178.78	0.5039	0.0500	-358.75	195.20	4.9628
6	$E_{batt,discharge}$	29.32	19.57	10.00	5.00	0.5000	0.1242	3.61	590.26	4.9609
7	$P_{peak,supply}$	31.57	161.47	18.45	348.58	0.8697	0.0908	149.90	268.40	4.6988
8	t_m	22.88	16.10	218.87	138.39	0.5634	0.1672	48.97	595.48	4.2494
9	E_{feed}	28.69	41.50	383.68	728.03	0.9282	0.1711	32.86	392.67	4.6852
10	$P_{peak,feed}$	22.99	351.10	226.85	469.36	0.9472	0.1074	-475.62	206.53	1.0618
11	(knee point 1)	6.33	254.21	145.55	596.61	0.9090	0.3607	-313.61	539.80	3.1487
12	(knee point 2)	27.06	209.21	243.38	918.93	0.5361	0.2591	60.78	396.57	4.3863

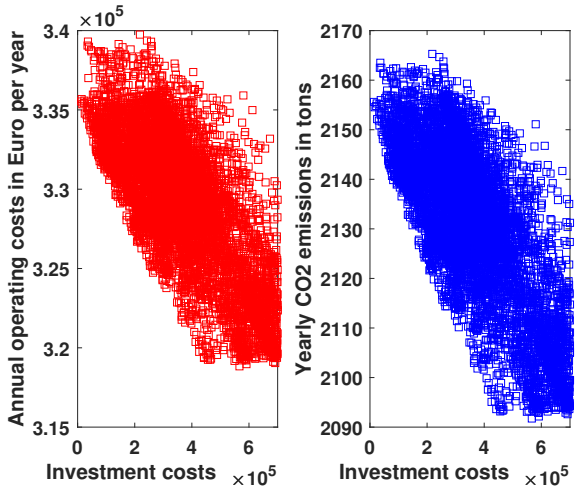

Fig. 12: Visualization of the relation between annual operational costs and the investment costs and the relation between investment costs and CO_2 emission using all non-dominated solutions obtained by REMO.

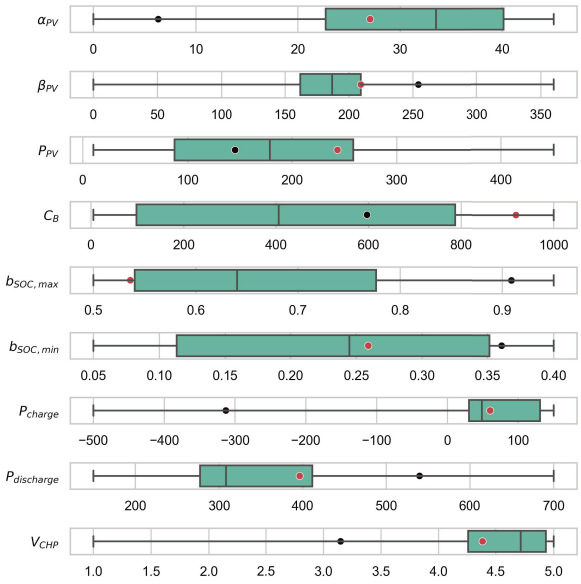

Fig. 13: Distribution of the decision variables for all Pareto non-dominated solutions: The boxes indicate the 25%-75% percentile, and the whiskers mark the minimum and maximum values. The markers indicate the two knee point solutions.

this analysis also shows that the overall savings potential for this specific use case are limited.

To better observe the quality of the solution set obtained by the six algorithms and provide domain experts with more informed knowledge of the optimal set and its boundaries for better decision-making, we also list the best-found solution by all runs for each objective and two of the knee solutions obtained by RVMM, as shown in Table III, and the corresponding parameters are listed in Table IV.

As a reference, the complete distributions of the decision variables and obtained objectives are shown in Fig. 13 and Fig. 14, respectively.

The first solution (id 1 in Table III) shows the lowest value for investment costs C_{invest}. The low investment costs are realized by utilizing a very small PV system (P_{PV}) and a very small battery capacity(C_B).

Solution 2, on the contrary, utilizes the largest possible PV system. In combination with a relatively large volume for the

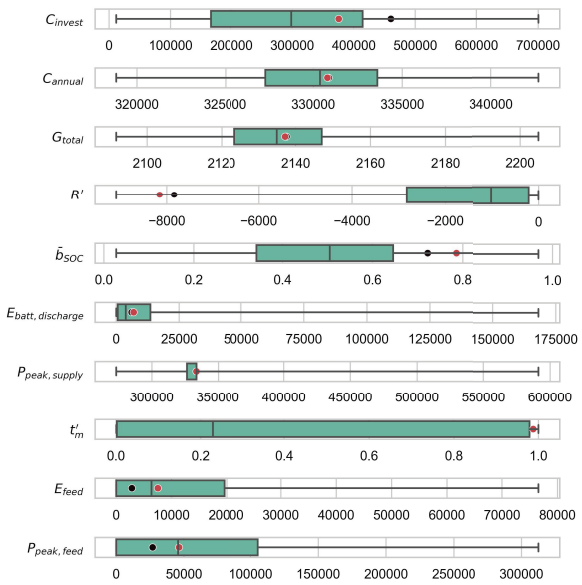

Fig. 14: Distribution of the objective values for all Pareto non-dominated solutions: The boxes indicate the 25%-75% percentile range, and the whiskers mark the minimum and maximum values. The markers indicate the two knee point solutions.

heat storage tank (V_{CHP}), it plausibly achieves the lowest annual costs (C_{annual}), illustrating the competitive nature of investment and annual costs. These two power sources provide more electricity than necessary for the building itself and feed a substantial amount into the grid (shown by high values for E_{feed} and $P_{peak,feed}$, in comparison to the low value of $E_{batt,discharge}$). By producing substantial amounts of energy from the large PV system and the CHP, the same solution is also able to achieve the lowest level of CO_2 emissions (G_{total}, see solution 3).

Solution 4 utilizes a large PV system in combination with a large battery. Together with the high mean state of charge (b_{SOC}) of the battery and its overall high charging limit ($b_{SOC,max}$), this results in the longest resilience time in cases when no grid power is available.

Solution 5 requires only a minimum battery SOC ($b_{SOC,max}$) and achieves the lowest mean battery state of charge.

Solution 6 utilizes the smallest possible PV system, as well as the smallest possible battery capacity and lowest maximum charging limit ($b_{SOC,max}$), thereby eliminating the utilization of the battery (shown by the lowest value of $E_{batt,discharge}$).

Solution 7 surprisingly achieves the lowest power peak demand from the grid ($P_{peak,supply}$), despite a very small PV system. The rather small battery (C_B) is efficiently discharged (shown by an above average value for $E_{batt,discharge}$) to compensate the demand peak. This behaviour is achieved with the highest possible battery charging threshold (P_{charge}) and a low discharging threshold ($P_{discharge}$). Overall, the solution seems to utilize the small battery very efficiently for power peak shaving. Interestingly, the solution does not rely on a large PV system to produce additional power when the building demand is high. Hence, an efficiently used battery seems to be more important for power peak shaving than a large PV system, in this specific scenario.

Solution 8 achieves the largest time share (t_m) in which the battery SOC is between 30% and 70% due to a combination of a low maximum battery SOC, high charging and high discharging thresholds. The battery has a mean state of charge of roughly 60%. Small charging or discharging processes are likely to keep the SOC between the desired values.

For solution 9, the lowest possible energy that is fed into the grid (E_{feed}) corresponds to a feed-in power peak value of zero and a high value for t_m. In spite of the large PV system, no excess energy is being produced and fed into the grid. This can be seen as a result of the low orientation angle of the PV system (β_{PV}). The orientation leads to an overall low energy production, in particular during times of higher energy demand around midday.

Solution 10 can be interpreted in a similar way. The high value for t_m and low value for E_{feed} are in line with the lowest possible feed-in power peak. The PV system is directed North, thus producing only a small amount of energy. Note that this is a very inefficient solution, indicating that multiple objectives are always needed to be considered.

Several insights into the optimization of the BEM problem can be further gained from the distribution of the decision variables and objectives of the Pareto non-dominated solutions (Figs. 13 and 14). While some decision variables, such as α_{PV}, P_{PV}, C_B, $b_{SOC,max}$, and $b_{SOC,min}$ take a wide range of values, β_{PV}, P_{charge}, $P_{discharge}$, and V_{CHP} can only take a small range of values to achieve good performance in all objectives. As expected, it can, for example, be observed that an orientation around 180° (South) is useful for the PV system, which is plausible considering a location in central Europe. It is unexpected, though very valuable, that mainly very large values for P_{charge} seem to have a positive effect on the optimization. This means that the stationary battery will be charged in most configurations, even for a net positive energy consumption, thus prioritizing the benefit that the battery provides over a potentially lower energy consumption. In a similar way, the results show that large values for V_{CHP} seem to be overall beneficial, highlighting the general advantage of a large heat storage volume. With regard to the objectives, it can be observed that most configurations lead to similar low values for $E_{batt,discharge}$ and $P_{peak,supply}$, with few exceptions.

Decision-makers may not have explicit preferences over the obtained solutions. In this case, it is suggested to choose knee points for implementation, as knee points can achieve a well-balanced trade-off between all conflicting objectives. As summarized in [49], there are three main commonly used knee identification methods. In this work, we propose using the convex knee based on the convex hull of the individual minima method to select the knee solutions. Since RVMM performs the best among the six algorithms under comparison, we propose selecting two of the most representative knee solutions from the solution set obtained by RVMM and have included them in Tables III and IV, as well as Figs. 13 and 14, respectively.

The knee points demonstrate the average performance for six of the objectives. They achieve very strong resilience values (R'), mainly due to the use of above average battery sizes (C_B) and high discharging thresholds ($P_{discharge}$). On the downside, this leads to above-average investment costs (C_{invest}) and a battery that is almost always charged with a high mean SOC (refer to t'_m and $\bar{b}_{SOC}$).

Another noteworthy aspect is the fact that, although the decision variables of both selected knee points take significantly different values, they lead to rather similar values in terms of objectives.

To summarize, the many-objective optimization algorithms can identify a set of optimal solutions. However, the task of selecting one single solution to be finally implemented is still the responsibility of the domain expert. Currently the most important benefit is that a more informed decision can be made given the knowledge of the optimal set and its boundaries. Nevertheless, further research is necessary for supporting the decision maker. Promising methods are currently being investigated, for example, incorporating human preferences into the decision making process [41], identifying solutions of interest from the Pareto set [50], directly integrating the user into an interactive multi-objective optimization [51], selecting knee points [49], or dividing the solutions into semantically meaningful concepts and selecting the representatives [52], [53].

VI. Conclusion

In this study, a real-world building energy management problem is formulated and then is optimized using a competitive multi-objective evolutionary algorithm and five surrogate-assisted evolutionary algorithms. A thorough analysis of the obtained solutions in terms of both the decision space and objective space is provided. Furthermore, it is suggested which timeout value should be set according to the amount of HV contribution in each time slot. The experimental results demonstrate that multi-objective SAEAs can be applied to identify a set of optimal solutions and are generally very helpful in improving the efficiency of building energy management. The performance of K-RVEA seems to be very close to RVEA-iGNG, indicating that better model management strategies need to be developed based on the properties of BEM to further improve performance and efficiency. In this work, by giving the knowledge of the optimal set and its boundaries, a more informed decision can be made to support decision-makers. However, which solution shall be finally implemented still requires the knowledge and preferences of domain experts.

Note that the time of each function evaluation ranges from less than one minute to more than two hours in the BEM. Thus, we believe it will be of great importance to include the cost of each real function evaluation when designing model management strategies, such as [14], to obtain competitive performance with the lowest cost. Thus, the proposed BEM problem can serve as a test problem for future design of new surrogate-assisted evolutionary algorithms or cost-aware Bayesian optimization, where expensive many-objective optimization problems are urgently needed. In our future work, we will design SAEAs by designing cost-aware model management strategies to select query points within the minimum time cost in light of this problem property of the BEM application.

References

[1] K. Deb, A. Pratap, S. Agarwal, and T. Meyarivan, "A fast and elitist multiobjective genetic algorithm: NSGA-II," *IEEE Transactions on Evolutionary Computation*, vol. 6, no. 2, pp. 182–197, 2002.

[2] K. Deb and H. Jain, "An evolutionary many-objective optimization algorithm using reference-point-based nondominated sorting approach, part I: Solving problems with box constraints." *IEEE Transactions on Evolutionary Computation*, vol. 18, no. 4, pp. 577–601, 2014.

[3] Q. Zhang and H. Li, "MOEA/D: A multiobjective evolutionary algorithm based on decomposition," *IEEE Transactions on Evolutionary Computation*, vol. 11, no. 6, pp. 712–731, 2007.

[4] R. Cheng, Y. Jin, M. Olhofer, and B. Sendhoff, "A reference vector guided evolutionary algorithm for many-objective optimization," *IEEE Transactions on Evolutionary Computation*, vol. 20, no. 5, pp. 773–791, 2016.

[5] X. Wang, X. Mao, and H. Khodaei, "A multi-objective home energy management system based on internet of things and optimization algorithms," *Journal of Building Engineering*, vol. 33, p. 101603, 2021.

[6] X. Li and A. Malkawi, "Multi-objective optimization for thermal mass model predictive control in small and medium size commercial buildings under summer weather conditions," *Energy*, vol. 112, pp. 1194–1206, 2016.

[7] F. Bre and V. D. Fachinotti, "A computational multi-objective optimization method to improve energy efficiency and thermal comfort in dwellings," *Energy and Buildings*, vol. 154, pp. 283–294, 2017.

[8] N. Kampelis, E. Tsekeri, D. Kolokotsa, K. Kalaitzakis, D. Isidori, and C. Cristalli, "Development of demand response energy management optimization at building and district levels using genetic algorithm and artificial neural network modelling power predictions," *Energies*, vol. 11, no. 11, p. 3012, 2018.

[9] T. Chugh, K. Sindhya, K. Miettinen, Y. Jin, T. Kratky, and P. Makkonen, "Surrogate-assisted evolutionary multiobjective shape optimization of an air intake ventilation system," in *2017 IEEE Congress on Evolutionary Computation (CEC)*. IEEE, 2017, pp. 1541–1548.

[10] T. Chugh, Y. Jin, K. Miettinen, J. Hakanen, and K. Sindhya, "A surrogate-assisted reference vector guided evolutionary algorithm for computationally expensive many-objective optimization," *IEEE Transactions on Evolutionary Computation*, vol. 22, no. 1, pp. 129–142, 2016.

[11] R. Cheng, T. Rodemann, M. Fischer, M. Olhofer, and Y. Jin, "Evolutionary many-objective optimization of hybrid electric vehicle control: From general optimization to preference articulation," *IEEE Transactions on Emerging Topics in Computational Intelligence*, vol. 1, no. 2, pp. 97–111, 2017.

[12] R. J. Lygoe, M. Cary, and P. J. Fleming, "A real-world application of a many-objective optimisation complexity reduction process," in *International Conference on Evolutionary Multi-Criterion Optimization*. Springer, 2013, pp. 641–655.

[13] E. J. Hughes, "Radar waveform optimisation as a many-objective application benchmark," in *International Conference on Evolutionary Multi-Criterion Optimization*. Springer, 2007, pp. 700–714.

[14] E. H. Lee, V. Perrone, C. Archambeau, and M. Seeger, "Cost-aware Bayesian optimization," *arXiv preprint arXiv:2003.10870*, 2020.

[15] G. Guinet, V. Perrone, and C. Archambeau, "Pareto-efficient acquisition functions for cost-aware Bayesian optimization," *arXiv preprint arXiv:2011.11456*, 2020.

[16] M. Abdolshah, A. Shilton, S. Rana, S. Gupta, and S. Venkatesh, "Cost-aware multi-objective Bayesian optimisation," *arXiv preprint arXiv:1909.03600*, 2019.

[17] T. Rodemann, "A comparison of different many-objective optimization algorithms for energy system optimization," in *Applications of Evolutionary Computation*, P. Kaufmann and P. Castillo, Eds. Springer, 2019, pp. 1–16.

[18] A. Jain, F. Smarra, E. Reticcioli, A. D'Innocenzo, and M. Morari, "NeurOpt: Neural network based optimization for building energy management and climate control," in *Learning for Dynamics and Control*. PMLR, 2020, pp. 445–454.

[19] M. H. Khan, A. U. Asar, N. Ullah, F. R. Albogamy, and M. K. Rafique, "Modeling and optimization of smart building energy management system considering both electrical and thermal load," *Energies*, vol. 15, no. 2, p. 574, 2022.

[20] S. K. Howell, H. Wicaksono, B. Yuce, K. McGlinn, and Y. Rezgui, "User centered neuro-fuzzy energy management through semantic-based optimization," *IEEE Transactions on Cybernetics*, vol. 49, no. 9, pp. 3278–3292, 2018.

[21] T. Rodemann, "A many-objective configuration optimization for building energy management," in *2018 IEEE Congress on Evolutionary Computation (CEC)*. IEEE, 2018, pp. 1–8.

[22] N. Delgarm, B. Sajadi, and S. Delgarm, "Multi-objective optimization of building energy performance and indoor thermal comfort: A new method using artificial bee colony (ABC)," *Energy and Buildings*, vol. 131, pp. 42–53, 2016.

[23] S. Mostaghim and J. Teich, "Strategies for finding good local guides in multi-objective particle swarm optimization (MOPSO)," in *Proceedings of the 2003 IEEE Swarm Intelligence Symposium. SIS'03 (Cat. No. 03EX706)*. IEEE, 2003, pp. 26–33.

[24] T. Murata, H. Ishibuchi *et al.*, "MOGA: multi-objective genetic algorithms," IEEE Piscataway, NJ, USA, pp. 289–294, 1995.

[25] Q. Xue, Z. Wang, and Q. Chen, "Multi-objective optimization of building design for life cycle cost and CO2 emissions: A case study of a low-energy residential building in a severe cold climate," in *Building Simulation*, vol. 15, no. 1. Springer, 2022, pp. 83–98.

[26] X.-k. Liang, Y. Zhang, and D.-w. Gong, "Surrogate-assisted multi-objective particle swarm optimization for building energy saving design," in *International Conference on Evolutionary Multi-Criterion Optimization*. Springer, 2021, pp. 593–604.

[27] Z. Yong, Y. Li-Juan, Z. Qian, and S. Xiao-Yan, "Multi-objective optimization of building energy performance using a particle swarm optimizer with less control parameters," *Journal of Building Engineering*, vol. 32, p. 101505, 2020.

[28] M. Moustapha, A. Galimshina, G. Habert, and B. Sudret, "Multi-objective robust optimization using adaptive surrogate models for problems with mixed continuous-categorical parameters," *arXiv preprint arXiv:2203.01996*, 2022.

[29] Y. Jin and B. Sendhoff, "A systems approach to evolutionary multi-objective structural optimization and beyond," *IEEE Computational Intelligence Magazine*, vol. 4, no. 3, pp. 62–76, 2009.

[30] Y. Jin, "Surrogate-assisted evolutionary computation: Recent advances and future challenges," *Swarm and Evolutionary Computation*, vol. 1, no. 2, pp. 61–70, 2011.

[31] D. R. Jones, M. Schonlau, and W. J. Welch, "Efficient global optimization of expensive black-box functions," *Journal of Global Optimization*, vol. 13, no. 4, pp. 455–492, 1998.

[32] Z. Song, H. Wang, C. He, and Y. Jin, "A kriging-assisted two-archive evolutionary algorithm for expensive many-objective optimization," *IEEE Transactions on Evolutionary Computation*, vol. 25, no. 6, pp. 1013–1027, 2021.

[33] D. Zhan, Y. Cheng, and J. Liu, "Expected improvement matrix-based infill criteria for expensive multiobjective optimization," *IEEE Transactions on Evolutionary Computation*, vol. 21, no. 6, pp. 956–975, 2017.

[34] Q. Zhang, W. Liu, E. Tsang, and B. Virginas, "Expensive multiobjective optimization by MOEA/D with Gaussian process model," *IEEE Transactions on Evolutionary Computation*, vol. 14, no. 3, pp. 456–474, 2009.

[35] Q. Liu, Y. Jin, M. Heiderich, and T. Rodemann, "Surrogate-assisted evolutionary optimization of expensive many-objective irregular problems," *Knowledge-Based Systems*, vol. 240, p. 108197, 2022.

[36] Q. Liu, R. Cheng, Y. Jin, M. Heiderich, and T. Rodemann, "Reference vector-assisted adaptive model management for surrogate-assisted many-objective optimization," *IEEE Transactions on Systems, Man, and Cybernetics: Systems*, vol. 52, no. 12, pp. 7760–7773, 2022.

[37] L. Pan, C. He, Y. Tian, H. Wang, X. Zhang, and Y. Jin, "A classification-based surrogate-assisted evolutionary algorithm for expensive many-objective optimization," *IEEE Transactions on Evolutionary Computation*, vol. 23, no. 1, pp. 74–88, 2018.

[38] Y. Yuan and W. Banzhaf, "Expensive multi-objective evolutionary optimization assisted by dominance prediction," *IEEE Transactions on Evolutionary Computation*, vol. 26, no. 1, pp. 159–173, 2021.

[39] H. Hao, A. Zhou, H. Qian, and H. Zhang, "Expensive multiobjective optimization by relation learning and prediction," *IEEE Transactions on Evolutionary Computation*, vol. 26, no. 5, pp. 1157–1170, 2022.

[40] H.-G. Huang and Y.-J. Gong, "Contrastive learning: An alternative surrogate for offline data-driven evolutionary computation," *IEEE Transactions on Evolutionary Computation*, 2022.

[41] T. Schmitt, M. Hoffmann, T. Rodemann, and J. Adamy, "Incorporating human preferences in decision making for dynamic multi-objective optimization in model predictive control," *Inventions*, vol. 7, no. 3, 2022. [Online]. Available: https://www.mdpi.com/2411-5134/7/3/46

[42] Q. Liu, Y. Jin, M. Heiderich, T. Rodemann, and G. Yu, "An adaptive reference vector-guided evolutionary algorithm using growing neural gas for many-objective optimization of irregular problems," *IEEE Transactions on Cybernetics*, vol. 52, no. 5, pp. 2698–2711, 2022.

[43] E. Zitzler and L. Thiele, "Multiobjective evolutionary algorithms: a comparative case study and the strength Pareto approach," *IEEE Transactions on Evolutionary Computation*, vol. 3, no. 4, pp. 257–271, 1999.

[44] H. Ishibuchi, R. Imada, Y. Setoguchi, and Y. Nojima, "How to specify a reference point in hypervolume calculation for fair performance comparison," *Evolutionary Computation*, vol. 26, no. 3, pp. 411–440, 2018.

[45] Y. Tian, R. Cheng, X. Zhang, F. Cheng, and Y. Jin, "An indicator-based multiobjective evolutionary algorithm with reference point adaptation for better versatility," *IEEE Transactions on Evolutionary Computation*, vol. 22, no. 4, pp. 609–622, 2017.

[46] R. Unger, B. Mikoleit, T. Schwan, B. Bäker, C. Kehrer, and T. Rodemann, "Green building-modeling renewable building energy systems with emobility using modelica," in *Proceedings of Modelica 2012 Conference*. Modelica Association, 2012.

[47] Y. Tian, R. Cheng, X. Zhang, and Y. Jin, "PlatEMO: A MATLAB platform for evolutionary multi-objective optimization," *IEEE Computational Intelligence Magazine*, vol. 12, no. 4, pp. 73–87, 2017.

[48] Y. Hua, Q. Liu, K. Hao, and Y. Jin, "A survey of evolutionary algorithms for multi-objective optimization problems with irregular Pareto fronts," *IEEE/CAA Journal of Automatica Sinica*, vol. 8, no. 2, pp. 303–318, 2021.

[49] G. Yu, L. Ma, Y. Jin, W. Du, Q. Liu, and H. Zhang, "A survey on knee-oriented multiobjective evolutionary optimization," *IEEE Transactions on Evolutionary Computation*, vol. 26, no. 6, pp. 1452–1472, 2022.

[50] T. Ray, H. K. Singh, K. H. Rahi, T. Rodemann, and M. Olhofer, "Towards identification of solutions of interest for multi-objective problems considering both objective and variable space information," *Applied Soft Computing*, vol. 119, p. 108505, 2022. [Online]. Available: https://www.sciencedirect.com/science/article/pii/S1568494622000503

[51] P. Aghaei Pour, T. Rodemann, J. Hakanen, and K. Miettinen, "Surrogate assisted interactive multiobjective optimization in energy system design of buildings." *Optimization and Engineering*, vol. 23, pp. 303–327, 2022.

[52] F. Lanfermann, S. Schmitt, and S. Menzel, "An Effective Measure to Identify Meaningful Concepts in Engineering Design optimization," in *2020 IEEE Symposium Series on Computational Intelligence (SSCI)*. IEEE, dec 2020, pp. 934–941.

[53] F. Lanfermann and S. Schmitt, "Concept identification for complex engineering datasets," *Advanced Engineering Informatics*, vol. 53, p. 101704, 2022.